| REPORT DOCUMENTATION PAGE | Form Approved OMB No. 0704-0188 |
|---|---|



| 1. REPORT DATE (DD-MM-YYYY) | 2. REPORT TYPE | 3. DATES COVERED (From - To) |
|---|---|---|
| 02/07/2006 | Final Technical Report | Feb. 15, 2003 - Dec. 31, 2005 |

**4. TITLE AND SUBTITLE**
Final Report for Excitation Models Grant Closing Dec. 2005

Project title, "Development of Models and Computational Tools for the Study of Space-Based Micro Propulsion Systems"

**5a. CONTRACT NUMBER**

**5b. GRANT NUMBER**
F49620-03-1-0144

**5c. PROGRAM ELEMENT NUMBER**

**6. AUTHOR(S)**
Deborah Levin, Associate Professor of Aerospace Engineering

**5d. PROJECT NUMBER**

**5e. TASK NUMBER**

**5f. WORK UNIT NUMBER**

**7. PERFORMING ORGANIZATION NAME(S) AND ADDRESS(ES)**
The Pennsylvania State University
110 Technology Center, 200 Innovation Blvd.
University Park, PA 16802

**8. PERFORMING ORGANIZATION REPORT NUMBER**

**9. SPONSORING/MONITORING AGENCY NAME(S) AND ADDRESS(ES)**
AF Office of Scientific Research, 4015 Wilson Blvd., Room 713,
Arlington, VA 22203-1954 /
Office of Naval Research, 230 S. Dearborn Ave., Rm. 380
Chicago, IL 60604-1595
Dr Mitat Birkan /NA

**10. SPONSOR/MONITOR'S ACRONYM(S)**
AFOSR / ONR

**11. SPONSOR/MONITOR'S REPORT**

AFRL-SR-AR-TR-06-0310

**12. DISTRIBUTION/AVAILABILITY STATEMENT**
Approved for public release; distribution in unlimited.

**13. SUPPLEMENTARY NOTES**

**14. ABSTRACT**

This final report presents the major technical accomplishments of this grant: 1) Implementation of a Kinetic Nucleation Model for DSMC, and 2) Use of Quasiclassical Trajectory Methods to Model OH Production Mechanisms in a Side-Jet RCS Flow. Specific technical details are provided in the actual report.

**15. SUBJECT TERMS**

| 16. SECURITY CLASSIFICATION OF: | | | 17. LIMITATION OF ABSTRACT | 18. NUMBER OF PAGES | 19a. NAME OF RESPONSIBLE PERSON |
|---|---|---|---|---|---|
| a. REPORT | b. ABSTRACT | c. THIS PAGE | | | 19b. TELEPHONE NUMBER (Include area code) |
| U | U | U | UU | 30 | |

Standard Form 298 (Rev. 8/98)
Prescribed by ANSI Std. Z39.18

20060727330

PENNSTATE

*Department of Aerospace Engineering*

# Inter-office Memorandum

| | |
|---|---|
| *TO* | Dr. Mitat A. Birkan |
| *FROM* | Deborah Levin, Assoc. Prof. of Aerospace Engineering |
| *SUBJECT* | Final Report for Excitation Models Grant Closing Dec. 2005 |
| *DATE* | 7 February 2006 |

This report presents the major technical accomplishments of the above mentioned grant. The report is subdivided into two sections that discuss the highlights of the research that has been performed.

## I. Implementation of a Kinetic Nucleation Model for DSMC

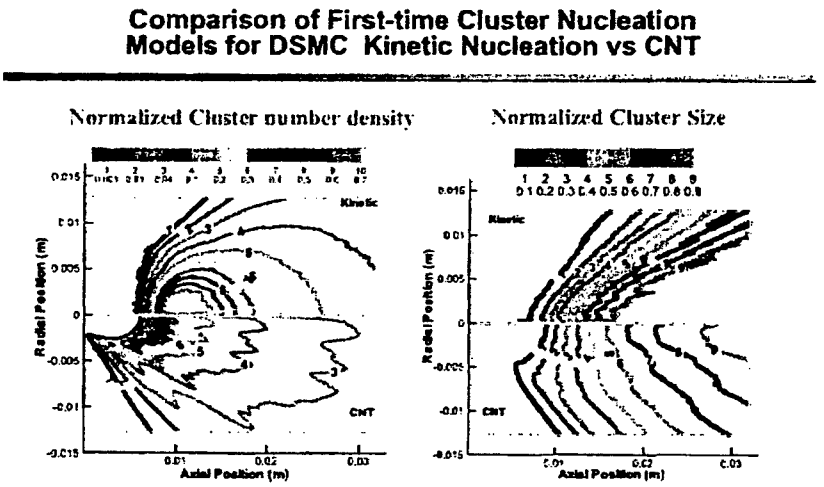


**Figure. 1**

1. Explanation of Figure 1

Cluster numbers and size distributions are shown for a simple expansion of an Argon gas into a vacuum through a sonic nozzle with a diameter of 3.2 mm, a stagnation temperature of 280 K, and a stagnation pressure of 125 torr. The clusters are formed during the non-equilibrium expansion through the process of homogeneous nucleation. Two sets of comparisons are presented for cluster number density and average cluster size, with the top contours showing the kinetic nucleation result and the bottom contours showing the results obtained from Classical Nucleation Theory (CNT). In the first comparison of cluster number density, the Kinetic and CNT results are normalized to 8 $x10^{20}$ and 8 x $10^{17}$ $m^{-3}$, respectively. In the comparison of the cluster size, on the right hand side, the contour levels are normalized to 50 and 1000 for the kinetic and CNT models, respectively.

The most important conclusion from the viewgraph is that there is a significant change in the physics of a homogeneous condensation flow depending on which cluster nucleation model is used. The kinetic nucleation process predicts three to four orders of magnitude more clusters are formed than CNT. Also, the kinetic nucleation model predicts that most of the clusters will be smaller than if the CNT is used. There are also important computational consequences when switching from the CNT to the kinetic nucleation model. The cluster size and number density contour distributions are smoother for the kinetic nucleation calculations even though both DSMC calculations have the same numerical parameters - number of gas and cluster particle $F_n$, number of cells and computational domain. The shakiness of the CNT contours is due to the necessity of obtaining the local gas temperature in order to calculate the nucleation rate. This is an inherently noisy process in a DSMC calculation.

Finally, these results are presented for Argon because there is a data base of laboratory measurements to which we can validate these results. This activity is in progress. When the method is extended to more realistic propellant mixtures of water and inorganic impurities, the amount of nucleation and the size of the clusters will affect plume signatures and the degree of backflow contamination.

2. Background explanations:

a. DSMC Implementation of cluster formation: A two-dimensional, axisymmetric DSMC simulation begins from the imposed starting surface, located at approximately one orifice diameter downstream of the orifice, and is composed of 45 jets. The entire DSMC computational domain is 4 by 10 orifice diameters squared, with 100 x 250 cells, each cell can be divided up to 16 subcells. The simulated vapor and cluster

particles represent $1.0 \times 10^{+10}$ and $5.0 \times 10^{+7}$ real particles respectively, and a total of about 860,000 simulated particles were used. A time step of $2.0 \times 10^{-9}$ sec is used with about 24,000 steps to reach the steady state and the simulation results are sampled for 200,000 steps.

b. Failure of CNT:

The DSMC/CNT has been successful in predicting average cluster properties for flows that exhibit very low amount of nucleation. However, it fails to predict cluster distribution properties. Since homogeneous condensation had never been incorporated directly into DSMC it was still a major advance to have a flow coupled condensation model. However, there are important problems with the inherent CNT assumptions when modeling, supersonic, expanding flows. CNT assumes that the initial clusters are born in a constant vapor environment and can only grow to a maximum size. The initial clusters, known as the critical clusters, are assumed to be born in an equilibrium isothermal vapor environment. The classical nucleation rate, $J$, is a function of macroscopic parameters as:

$$J = \sqrt{\frac{2\sigma}{\pi m^3}} \frac{\rho_v^2}{\rho_w} \exp\left(\frac{-4\pi r^2 \sigma}{3kT}\right)$$

where $\sigma$, the cluster surface tension and $\rho_w$, the cluster mass density, are the most problematic terms for small clusters.

c. Implementation of a full kinetic nucleation model: The molecular dynamics (MD) approach was used to simulate a 1-D Argon condensation plume along the centerline. A geometry criteria and history tracking method were used to analyze how the clusters are created in the plume and it was validated that the initial dimers were created through triple collision processes, during which the third monomer takes away the additional energy. The triple collision can be expressed as,

$$A + A + A \xrightarrow{k_f} A_2 + A$$

A and $A_2$ are atoms and stable dimers and

$$nk_f = \overline{\sigma c_r} \int_0^\infty P_t(E_t) f\left(\frac{E_t}{kT}\right) d\left(\frac{E_t}{kT}\right)$$

where $P_t$ is the probability of creating a stable dimer from a triple collision and $f$ is the energy equilibrium distribution function.

To be implemented into a DSMC scheme, the triple collision is decomposed into two successive binary collision steps:

$$A + A \rightarrow A_2^*$$

$$A_2^* + A \rightarrow A_2 + A$$

where $A_2^*$ is a temporary collision complex with a lifetime. Complex-monomer collisions are referred as the triple collisions. In the full DSMC simulation, we need both $P_t$ and the collision complex lifetime. A Hybrid DSMC/MD technique was employed to obtain $P_t$ in the full DSMC simulations. In addition, the acceptance-rejection principle is used to determine whether a binary collision occurs. Each successful binary collision $\Rightarrow$ a temporary complex. During the complex lifetime, complex-atom pairs are selected and the acceptance-rejection principle is applied assuming a hard-sphere like interaction between clusters and Argon atoms. The collision outcome is evaluated according to the probability, $P_t$, and a "successful" complex-atom collision generates a stable dimer. Subsequent cluster evolution processes, starting from dimers, are calculated using the previously developed models for cluster sticking and evaporation.

## II: Use Of Quasiclassical Trajectory Methods To Model OH Production Mechanisms In A Side-Jet RCS Flow

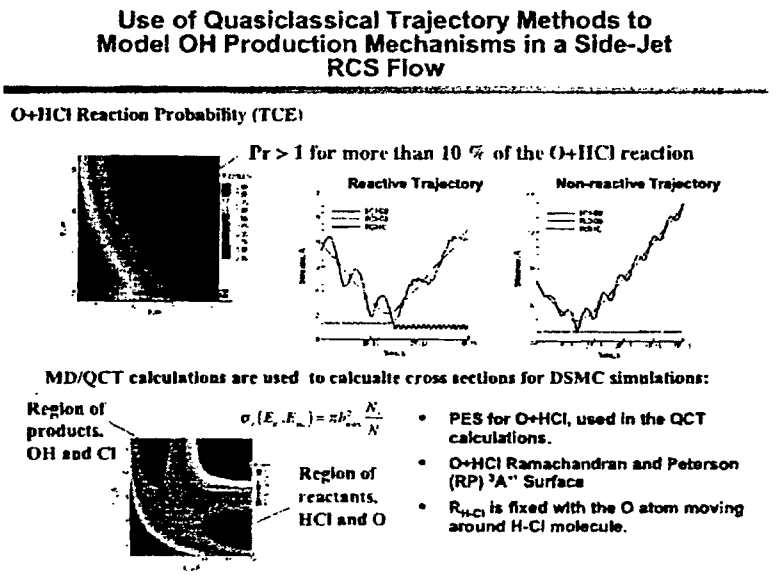


Figure 2.

1. Explanation of viewgraph:

The objective of this work is to understand why the common, readily available Total Collisional Energy (TCE) model for chemical reactions in DSMC fails for the exchange reaction of O+HCl → OH+Cl. This is an important chemical reaction occurring between the efluents of a solid-non-aluminized reaction control systems (RCS) and free stream atomic oxygen present in large quantities. Initial investigations of this multi-scale, chemically reacting flow showed that using the baseline TCE model approximately 10% of the reaction probabilities would be unphysically greater than unity, if an artificial limiter was not utilized in the calculations. For this reason we propose to develop a new chemical model that will be valid for chemically reactive, hypervelocity collisions.

We use the Quasi-Classical Trajectory/ Molecular Dynamics method (QCT/MD), an accurate chemical modeling tool, to evaluate the reaction and total collision cross sections. In this manner we can determine whether it is possible to propose a correction to the TCE model and we investigate the sensitivity of the full DSMC simulation to the different chemical models for this reaction for a hypersonic condition of 120 km altitude, 5 km/s, a typical free stream condition where these flows occur.

Background explanations:

The classical Hamiltonian is H=T+V=E, where T, and V are the kinetic and potential energy of the molecular system and Hamilton's equations of motion are

$$\dot{p}_{ij} = -\frac{\partial V}{\partial r_{ij}}, \dot{r}_{ij} = \frac{p_{ij}}{m_i}$$

where i=1,2,3 (atoms), j=1,2,3 (x,y,z); $p_{ij}$ and $r_{ij}$ are the Cartesian momenta and coordinates, and $m_i$ is the mass of the i-th atom. We solve the 18 coupled equations for $p_{ij}$ and $r_{ij}$ using a 4th-order Runge-Kutta method. To construct the initial conditions for each trajectory (i.e., internal energy of target HCl, relative velocity of O+HCl, offset or impact parameter), we use the micro-canonical sampling to obtain the initial conditions of the scattering event:

$$W = \sqrt{(E_{\text{int}} - V(R))}, p_{i,j} = fRn_{i,j}\sqrt{m_i} \quad i,j = 1,3$$

where V(R) is the potential energy surface (PES) shown on the viewgraph.

To obtain final state distributions of product, we assume that the vibrational and

rotational energies may be treated classically and separable. Each trajectory outcome is analyzed with the following classical relationships for angular momentum and vibration.

$$L = \mu R \times \dot{R}, J = -\frac{1}{2} + \frac{1}{2}\sqrt{\left(1 + 4\frac{L^2}{\hbar^2}\right)}, E_J = J(J+1)\frac{\hbar^2}{2\mu R_{eq}^2}. v = -\frac{1}{2} + \frac{2\mu}{h}\int_{R_<}^{R_>} \dot{R} dR$$

The conclusions of this work is that both the reaction and total cross sections, $\sigma_r$ and $\sigma_T$ , for O+HCl obtained using the MD/QCT method affected the OH production. Furthermore it was found that $\sigma_T$ was independent of the HCl internal energy and the usual Variable Hard Sphere (VHS) model used in DSMC could be corrected for high-temperature O-HCl collision pairs if VHS parameters of $w$=0.39, $d_{ref}$=3.9 Å at 1000 K are used. The most accurate reaction probability calculated by the QCT/MD method, $Pr$(MD), was less than 0.4 at 120 km altitude for freestream velocity of 5km/s.

The use of the MD/QCT model is limited by the accuracy of the PES and it is not typical that such high fidelity PESs are available. For this reason, the MD/QCT calculations were repeated for the older, more readily available, but less accurate, PES known as a LEPS. These surfaces could be more easily obtained for other propellants-atomic oxygen collisions. We are presently analyzing the results and how they affect the total OH production in the complete DSMC simulation.

AIAA 2005-0767

# A Kinetic Model of Condensation in a Free Argon Expanding Jet

Jiaqiang Zhong
The Pennsylvania State University
University Park, PA, 16802

Michael I. Zeifman
The Pennsylvania State University
University Park, PA, 16802

Deborah A. Levin
The Pennsylvania State University
University Park, PA, 16802

**43rd AIAA Aerospace Science Meeting**
Jan. 10 - 13, 2005 / Reno, Nevada

AIAA 2005-0767

# A Kinetic Model of Condensation in a Free Argon Expanding Jet

Jiaqiang Zhong* Michael I. Zeifman† Deborah A. Levin‡
*Pennsylvania State University, University Park, PA 16802*

## Abstract

The direct simulation Monte Carlo (DSMC) method has recently been developed to simulate homogeneous condensation in a free expansion rocket plume. However, cluster-monomer and cluster-cluster collision models as well as the determination of cluster size were simplified in the previous work which may greatly impact the accuracy of numerical simulation results. In this work, the molecular dynamics (MD) method is used to simulate collision and sticking probability for Ar clusters. The Ashrigz-Poo model is used to predict the outcome of cluster-cluster collisions. These improved models are then integrated into a DSMC code to predict the Rayleigh scattering intensity in a free expanding Argon condensation plume and numerical results are compared with experimental data along the plume centerline.

## 1 Introduction

Homogeneous condensation [1], observed in various types of plumes expanding into a vacuum, may result in contamination of spacecraft surfaces as well as affect the observance of high altitude plumes [2][3]. Extensive experimental studies on the condensation in real thrusters and small free-expanding jets have been conducted since the 1970's [4][5]. However, it is difficult to measure cluster size and number density distributions in an operational plume. Therefore a prediction tool which can be validated with small thruster data will provide crucial information about homogeneous condensation in typical chemical rocket plumes.

Most of the numerical work on condensation coupled to a gas expansion models the processes in ground-based facilities and uses continuum approaches [6]. Since free-expanding jets are mostly in the transitional to rarefied regimes, a continuum approach would be inapplicable to simulate condensation in a free expansion plume. Thus, a more appropriate kinetic approach should be used. Such an approach must address the processes of cluster nucleation, growth, decay and collisions with other clusters and monomers as well as the usual gas kinetics and is, therefore, computationally challenging.

Recently, the direct simulation Monte Carlo (DSMC) [7] method has been applied to simulate homogeneous condensation in free-expansion plumes [8][9]. The previous work [8] can be summarized as follows. Classical nucleation theory (CNT) [1] was used to model

*Graduate student, Department of Aerospace Engineering, AIAA student member.
†Research Associate, Department of Aerospace Engineering, AIAA member.
‡Associate Professor, Department of Aerospace Engineering, AIAA Associate Fellow.

the generation of initial nuclei, which are assumed to be created at the local critical conditions. Microscopic models, consistent with CNT theory, have been developed from general conservation equations to model sticking and non-sticking collisions, as well as evaporation processes. These models were then integrated into the DSMC method to simulate condensation coupled flow. The developed DSMC condensation model was numerically validated by comparing the simulation results with analytical solutions in one dimensional test cases, further validated by comparison with Hagana's scaling laws [4], and finally applied to predict water homogeneous condensation in a rocket plume.

In the previous work [8], clusters were modeled as hard spheres, with radius proportional to $i^{\frac{1}{3}}$, where $i$ is the number of molecules in the cluster. The probability of a sticking collision between a cluster and a condensible monomer was simply assumed to be unity [8] or 0.1 [9] without validation. Cluster-cluster collisions were assumed to be elastic without any allowance for coalescence, although it was shown that for cases considered in Ref. [8] the number of cluster-cluster collisions was small. Thus, there is room for improvement of the previous numerical simulations. The purpose of this work is to improve the fidelity of the models used in the condensation flow by use of the molecular dynamics (MD) method.

The paper is organized as follows. To understand basic cluster model and interactions between a cluster and a molecule, we choose a molecular dynamics [10] (MD) approach to simulate cluster-molecule collision and sticking processes in Sec. 2. In order to derive general conclusions from MD simulations, a 6-12 Lennard-Jones potential, applicable to many species, is used to simulate collision processes between Argon clusters and Argon monomers. Using reduced units, the MD simulation results of Argon species are compared with those of nickel from Ref. [11]. In Sec. 3, we briefly review the microscopic models developed in our previous work [8] and explain the similarities and differences of the previous model with the corrected models. These models are then used in Sec. 4 to simulate a condensation plume in the direct simulation Monte Carlo (DSMC) method of a free expanding Argon plume through a sonic orifice. Using the DSMC results, the Rayleigh scattering intensity is then calculated and compared with experimental data along the plume centerline [15].

# 2 Molecular Dynamics Simulation

## 2.1 Methodology

Molecular dynamics (MD) is a computer simulation technique which allows one to predict the time evolution of a system of interacting particles, e.g., atoms or molecules. Each real atom in MD is usually modeled as a point-size particle, and the interaction between them is modeled by an interaction potential. Once the system initial conditions are defined in terms of particle coordinates, and velocities, the system evolution in time is followed by solving the Hamilton equations.

The traditional 6-12 Lennard-Jones potential, valid for interactions among many species, is chosen as the interaction potential:

$$V = 4\varepsilon \left[ \left(\frac{\sigma}{r}\right)^{12} - \left(\frac{\sigma}{r}\right)^{6} \right] \qquad (1)$$

where the potential parameters for Argon are $\epsilon = 0.0103$ eV and $\sigma = 3.405$ Å . Note that in this section, we specifically focus on the interactions among Argon atoms.

Trajectories are integrated numerically using the Nordsieck fifth-order predictor-corrector algorithms [10], which can be summarized as follows. First, new positions as well as time derivative terms up to fifth order are predicted

at a new time step using a Taylor series expansion. Then, the force acting on each particle is computed for the predicted positions, and error terms are calculated by comparing force terms between the previous and current time steps. Finally, the above error terms are used to correct the particle positions and derivatives for the next time step.

## 2.2 Initial Clusters

To simulate cluster collision outcomes using a molecular dynamics approach, the initial conditions (coordinates and velocities) of each molecule within a cluster must be specified before the simulation. The condition of dimers, obtained from previous modeling of a free expansion plume [12], will be used to characterize the initial clusters for the MD simulations discussed in the subsections 2.3 and 2.4.

To explore the physics of the cluster formation processes in an expanding plume, a molecular dynamics approach was used to simulate a free argon expansion along the core plume. One challenge in the MD modeling of such a system is the selection of a criterion to distinguish clusters, especially dimers, from atoms that are just collision pairs. The Stillinger criterion [13] and a history tracking approach were used to find stable clusters as follows. First, the collision duration time between two atoms were simulated by the MD approach for conditions of various impact parameters and relative velocities, and the MD results were compared with Bunker's approximate formula[14]. It was found that the molecular collision duration time is usually less than 10ps. Then each molecular position in the plume was output every 10ps during the MD simulation, and a pure geometric Stillinger criterion was used to identify the clusters in the plume. In this way, the observed clusters were tracked using the MD output, i.e., every 10ps, until the atoms in the clusters had separated into monomers. We found that the dimer's lifetime could last more than 30ps in the plume, and they usually originated from a tri-atom collision process during which one of the atoms takes away extra energy, while the other two form a stable dimer.

To evaluate the cluster cross section and cluster-monomer sticking probabilities, we also need to prepare clusters of size greater than two for cluster configurations, typical of expanding flows. Trimers were created through a dimer-monomer sticking collision, tetramers through trimer-monomer sticking collisions, and so on. To efficiently generate larger clusters, cluster-cluster sticking collisions may be used.

Molecular dynamics simulation results of cluster-monomer collisions will be discussed in the following subsection 2.3 and 2.4. Each MD simulation case is repeated for various trajectories by randomly rotating the initial cluster around its center of mass and the results averaged over the trajectories are shown in the subsections 2.3 and 2.4.

## 2.3 Cluster Model

The cluster-monomer collision process may be used to define the cluster cross section, as the monomer-monomer collision defines molecular cross section in the traditional DSMC approach. To characterize the cluster model, the collision processes of cluster-monomers are simulated with the MD method, under the condition of various impact parameters, $b$, and relative velocities, $v_{rel}$. Sticking collisions are obviously counted as effective collisions, while for non-sticking collisions, only trajectories in which the deflection angle is at least 10 degrees are counted as collisions. Note that the colliding molecules are initially separated sufficiently far from the target cluster such that the effective interaction potential between them is zero.

The collision probability for each case ($b$, $v_{rel}$) is defined as the ratio of the number of

trajectories that resulted in a collision to the total number of trajectories. For each case, a sample of 200 trajectories is used with the orientation of the target cluster to the monomer randomly chosen. The impact parameter $b$ increases from a head-on collision value of zero to a value in which the cluster-monomer collision probability is close to zero. Relative collision velocities from approximately 150 to 225 $m/s$ are chosen, and the cluster sizes selected for study in the MD simulations ranges from a dimer up to 482-mers. The range of cluster size and collision impact parameter are typical in a condensation flow [8], and the collision relative velocity corresponds to a translational thermal temperature which is also representative of a typical nondimensional temperature, the ratio of the collision thermal temperature to the species freezing temperature.

Representative MD simulation results are shown in Fig. 1. It can be seen that the collision probability is close to unity for the cases with relatively small impact parameter. For the cluster collision probability of dimer-monomer collisions, for example, it can be seen that for impact parameters $b$ less than $b_s \approx 7.5$ Å , the probability is almost independent of the impact parameter $b$. For collisions with $b$ greater than $b_s$, the collision probability decreases rapidly to zero as the impact parameter increases. It can also be seen that $b_s$, defined as the critical impact parameter, increases as the cluster size increases.

The maximum impact parameter $b_m$, chosen here to correspond to a collision probability of 0.1, can be used to calculate the cluster-monomer collision cross section, $\sigma$, as $\sigma = \pi b_m^2$. It is related to the cluster and monomer diameters as [7]

$$b_m = \frac{d_c + d_0}{2} \tag{2}$$

where $d_c$ and $d_0$ are the cluster and molecule diameters, respectively. Thus, the cluster radius, $R_i = \frac{d_c}{2}$, can be determined from the MD simulation results, since the monomer diameter is known. The MD results are shown in Fig. 2 with a relative collision velocity of $182m/s$ and are fitted to an analytic general cluster radius equation [16]:

$$R_i = Ai^{\frac{1}{3}} + B \tag{3}$$

where $i$ is the number of molecules in the cluster, and $A$ and $B$ are constants. It can be seen that the MD simulation results for Argon clusters fit this equation quite well by choosing $A$ 2.3Å and $B$ 3.4Å (dashed line in Fig. 2).

The molecular dynamics simulations also show that cluster-monomer collision probabilities are a function of the relative collision velocities. Results of collision probabilities for different cluster sizes and relative cluster monomer velocities are shown in Fig. 3. It can be seen that the critical impact parameter increases as the relative collision velocity decreases, and therefore, the cluster cross section would also increase as the relative velocity decreases. To model the dependence of cluster diameter on the relative collision velocity $c_r$, we use the variable hard sphere (VHS) [7] model

$$d = d_{ref}(\frac{c_{ref}}{c_r})^{\nu} \tag{4}$$

where the subscript $_{ref}$ refers to a reference value and $\nu$ is a constant related to species viscosity. The MD results for cluster radii, calculated for various relative collision velocities, are shown in Fig. 4, and the simulation results fitted to Eq. (4) are shown as dashed lines. Figure 4 shows that the cluster radii are approximately inversely proportional to the relative collision velocity, and the slopes for different cluster sizes are similar. The reference cluster diameter, $d_{ref}$, may be estimated from Eq. (3). For larger cluster size, the $d_{ref}$ is higher so that a smaller $\nu$ is required to correct its diameter for the impact of relative collision velocity. It can be seen that as the cluster size increases from dimer to 147-mers, the constant $\nu$ decreases approximately from 0.3 to 0.07. Note that for Argon vapor, the constant $\nu$ is about

0.31. Thus, the impact of collision relative velocity on the cluster cross section becomes less as the cluster size increases, which indicates that the hard sphere model may be used to model relatively large clusters in the DSMC simulation. As Fig. 4 shows, the error in using the hard sphere model increases for small clusters.

## 2.4 Sticking Collision Probability

The sticking probability for a collision process between a cluster and a molecule can be simulated in a manner similar to the collision probability. Initially, the target Argon cluster is at the origin in a static state[1], while the colliding Argon atom is approximately 50 Å away from the cluster. It takes about 25 ps before the atom collides with the target cluster. The simulation time for a colliding case is approximately 100 ps, which is also long enough to observe whether the outcome is a sticking or non-sticking collision. To get good statistics, we perform 2500 trajectories for each colliding case by randomly rotating the target cluster, as discussed in Sec. 2.3.

It can be expected that cluster-monomer sticking probability is also dependent on the relative collision velocity, especially for small clusters. Similarly to the collision probability, the impact of the relative velocity on the sticking probability decreases as the cluster size increase. Figure 5 shows the MD simulation results of sticking probabilities for various cluster sizes and relative velocities as a function of impact parameter. This figure indicates that the sensitivity of the sticking probability decreases as the cluster size increases, and it may be neglected for the clusters larger than 10-mers with good approximation. To highlight the size dependence of the sticking probability, Fig. 6 shows the sticking probability as a function of impact parameter for different size clusters all with a relative collision velocity of $182m/s$. It can be seen that the sticking collision probability, similar to the collision probability, exhibits a critical impact parameter dependence. For collisions with impact parameters less than the critical impact parameter, the sticking probabilities are almost constant, and are unity for cluster sizes larger than 10-mers. While for collisions with impact parameters larger than the critical impact parameter, the sticking probabilities decrease to zero more quickly than the collision probabilities. As can be seen from Fig. 6, the critical collision impact parameter for the sticking collision probability increases as the cluster size increases.

In the DSMC simulation of an expanding flow, consisting of gas and clusters, each collision is not modeled in detail and only average collision properties are used. For this reason, the dependence of the sticking probability on impact parameter must be averaged over the collision cross section. The average sticking probability, $P^i_{av}$, can be calculated from the MD results for each cluster based on a $b^2$ distribution of collision pairs,

$$P^i_{av} = \frac{1}{b^2_{i,m}} \int_0^{b_{i,m}} P(b)\, db^2 \qquad (5)$$

where $b_{i,m}$ is the cluster maximum impact parameter or collision radius, given by Eq. (2). Figure 7 shows the averaged sticking probability, $P^i_{av}$, as a function of cluster size for a relative collision velocity of $182m/s$. It can be seen that for cluster size smaller than 10, the sticking collision probability increases quickly as the cluster size increases; while for cluster size larger than 10, the sticking collision probability is independent of cluster size and is very close to unity.

Therefore, the MD simulation results show that for clusters larger than 10-mers, cluster-monomer interactions may be modeled approx-

[1] A static state indicates one with no translational velocity, and only thermal motion or internal energy.

imately with the hard sphere model, with a constant sticking coefficient of unity. The MD simulation study confirms the selection of these models utilized in earlier work [8].

## 2.5 Comparison of MD results for different Lennard-Jones Systems

Collision processes between argon clusters and molecules have been simulated in the previous sections, and important results of cluster size and sticking coefficients are shown in Fig. 2 and Fig. 7 respectively. Since Lennard-Jones potential is generally used to describe molecular interaction for many other species, the simulated results for Argon may be able to roughly estimate other species without conducting numerically identical simulations using various parameters. To validate our MD simulations, we would like to compare our numerical results with other independent data [11].

Nickel cluster collision cross sections and sticking collision process has been simulated by the MD method in the Ref. [11], using a Lennard-Jones potential. First we may directly compare Ni and Ar cluster sticking probabilities, which is a nondimensional parameter. Note that the nickel cluster sticking probability is defined as the ratio of the cluster sticking cross section to the total cross section and both quantities are given in Ref. [17]. The comparison of Argon and Nickel cluster sticking probability is shown in Fig. 7, represented by open circles and solid triangles respectively. Figure 7 suggests that the trends for small cluster sticking probability discussed in Sec. 2.4 is similar for both argon and nickel clusters.

To compare cluster collision cross sections for different species, we have to use reduced units to analyze the MD simulation results of Ref. [17]. We assume that the cluster cross section radius can be expressed as:

$$r_i + r_1 \propto \sigma f(\epsilon, m) \propto \sigma \frac{\epsilon^p}{m^q} \qquad (6)$$

where $r_i$ is the radius of a cluster consisting of $i$ monomers, $r_1$ is the monomer's radius, $\sigma$ and $\epsilon$ are the Lennard-Jones parameters, $m$ is the molecular mass, and $p$ and $q$ are constants.

The nickel cluster cross sections are simulated in Ref. [11] with two Lennard-Jones potentials, the bulk fitted (LJB) and dimer fitted (LJD) potential. The simulation results for clusters of size from dimer to 13-mers are given in Ref. [11], e.g. a 12-mers cluster cross section is about 250 Å $^2$ for the LJB potential, and 200 Å $^2$ for the LJD potential. The constant $p$ in Eq. (6) can be estimated by comparing those two simulated 12-mers cross sections and was found to be approximately 0.18. Examination of Fig. 2 shows that, the 12-mers argon cluster cross section is approximately 363 Å $^2$ which compared with the Nickel cluster computed with the LJB potential, allows one to estimate a $q$, value of approximately 1.56.

By using Eq. (6), the Argon cluster collision cross sections can be used to predict nickel cluster collision cross sections. A comparison of the Ar derived predicted Ni cross sections with those obtained in Ref. [11] is shown in Fig. 8. It can be seen that the argon cross sections can predict nickel cluster cross sections well for both Ni interaction potentials. Thus, the Argon cluster sticking probability and collision cross section are consistent with those of nickel clusters, and these results may be extended in the future to approximately estimate other species described by theLennard-Jones potential, such as water.

# 3 Microscopic Models

Based on the general conservation equations, the developed microscopic models had been integrated into a DSMC computational scheme to predict homogeneous condensation in a

rocket plume. Detail descriptions of these models can be found in the previous work [8]. To predict Argon condensation in a free expanding plume in Sec. 4, we briefly review these models, and discuss the improvements in detail as follows.

## 3.1 Simulated Molecular Models

To simulate condensation coupled flow, all species including monomers and clusters are represented by simulated molecules in the DSMC approach. The variable hard sphere (VHS) model is used to model simulated molecules representing real atoms or molecules in the plume, and the Larsen-Borgnakke model is used to redistribute molecule-molecule collision energy, based on the number of degrees of freedom. Note that both rotation and vibration energy transfer are considered in molecule-molecule collisions.

An analytic cluster hard sphere model is described in Ref. [16], providing a general asymptotical equation for cluster radius similar to Eq. (3). Briehl *et al* [19] applied this cluster model to simulate small Cu cluster growth and decay processes using the DSMC approach. This cluster model has been validated by our MD simulations for Argon cluster, discussed in Sec. 2.2. It was further shown that Argon cluster model is consistent with other independent studies of Nickel clusters [11] in Sec. 2.5. Thus, we will use the hard sphere cluster model in our DSMC simulation.

## 3.2 Nucleation Model

Following CNT theory, initial clusters, called nuclei, are introduced into the computational domain. The nuclei have the same size as the local critical clusters, and they are in an equilibrium state with the surrounding gas. The nucleation rate, $J$, is given in the CNT theory as:

$$J = \left(\frac{2\sigma}{\pi m^3}\right)^{\frac{1}{2}} \frac{\rho_v^2}{\rho_w} \exp\left(-\frac{4\pi r_*^2 \sigma}{3k_B T}\right) \quad (7)$$

where $\sigma$ is the cluster surface tension, $m$ is molecular mass, $\rho_v$ is vapor density, $\rho_w$ is cluster density, and $r_*$ is the local critical cluster radius. Thus, during a time step $\Delta t$ in a cell with volume $\Delta V$, the number of new simulated nuclei $N_c$ is calculated as

$$N_c = J_c \Delta V \Delta t / F_c \quad (8)$$

where $F_c$ is the number of real molecules represented by a simulated cluster molecule. The latent heat, generated during the nucleation process, is distributed to the ambient gas molecules in a cell according to energy equipartition principle. Using the bulk theory, the latent heat, $E_L$, is given by

$$E_L = LM_i \quad (9)$$

where $L$ is the specific latent heat of evaporation, and $M_i$ is the mass of a cluster consisting of $i$ monomers.

## 3.3 Collision Models

The collision process between a cluster and a foreign molecule is referred to as non-sticking collisions, while the outcome of a collision between a cluster and its own molecule may be sticking, or non-sticking, depending on the sticking collision probability. Based on molecular dynamics simulations, a general expression for both argon and water homogeneous sticking coefficient, $q$, has been summarized as[21]

$$q = \left(1 - \sqrt[3]{\frac{V^l}{V^g}}\right) \exp\left(-\frac{E_o}{K_B T}\right) \quad (10)$$

where $V^l$ and $V^g$ are the specific volumes of gas and liquid and $E_0$ is the energy difference of the minimum quantum level between the activated

complex and gas. Equation (10) shows that sticking coefficient is close to unity in the low temperature region and decreases as the temperature increases. As shown in our MD simulations, sticking coefficient for clusters smaller than 11-mers may not agree with the prediction of Eq. (10) since it is based on the condition of a flat liquid surface. The impact of correctly modeling the sticking probability of clusters smaller than 11-mers on the condensation results will be discussed in Sec. 4.

In the previous work, cluster-cluster collisions are assumed to be elastic collision, without considering the coalescence effect. In this work, the semiempirical Ashgriz-Poo model[22] is chosen to predict the outcome of cluster-cluster collisions that may lead to coalescence or separation. The Weber number, defined as the ratio of collision kinetic energy to droplet surface energy, provides a cluster-cluster collision separation-coalescence boundary. The Weber number, $We$, is given by:

$$We = \frac{\rho_d d_i c_r^2}{\sigma_d} \tag{11}$$

where $\rho_d$ is the cluster density, $d_i$ is the diameter of the smaller cluster, $c_r$ is the cluster-cluster relative velocity, and $\sigma_d$ is the cluster surface tension. The Ashgriz-Poo model has been verified for water droplets by MD simulations using a 6-12 Lennard-Jones potential, and was used to predict the outcome of droplet collisions in an inductively coupled plasma [23]. The detail description of the Ashgriz-Poo model can be found in Ref. [22].

# 4 Results and Discussions

The MD simulation results, cluster collision cross sections and cluster-monomer sticking coefficients, will be integrated into the DSMC simulations. To understand the impact of these improvements and check the simulation results presented in the previous work [8], we want to first compare the improved DSMC simulation results with previous results.

A free argon expanding flow through a sonic nozzle with a convergent angle of 30 degrees into a vacuum environment was simulated in Ref. [8]. The plume has a stagnation pressure of $5.30 \times 10^4$ Pa, and a stagnation temperature of 180 K. The DSMC simulation parameters and techniques for this case were described in detail in Ref. [8]. Comparisons between improved (new) and previous results (old) are shown in Fig. 9. Since the MD corrected cluster-monomer collision cross sections are larger than the previous ones, the comparison of average cluster size, shown in the top of the figure, suggests that the cluster size obtained by the improved model is larger than the previous size. However, after the cluster size is normalized to the corresponding terminal cluster size, the middle figure of Fig. 9 shows that the normalized curves of the improved and previous models are almost the same. The middle figure suggests that the improved model still validates the scaling laws of Hagena [4], as was shown in the previous work [8]. Finally, the cluster number densities are compared in the bottom of Fig. 9 and the results suggest that the cluster number density obtained by the improved model is slightly less than the previous value. The main reason of the decreased cluster number density is that small clusters in the improved model have had more chance to evaporate into separate atoms due to relative smaller sticking coefficients.

Next, the improved condensation model is applied to a new expanding condensation plume experimentally studied in the Arnold Engineering Development Center (AEDC) in the 1970's [15]. Extensive sets of Rayleigh scattering intensity data were measured, which may be directly compared with numerical results. A brief summary of the scattering intensity is given below and detail information can be found in Ref. [15].

Assuming that the condensing flow field

is composed of a collection of gas phase monomers and i-mers with the respective number density $N_i$ and polarizability $\alpha_i$, the ratio of scattered intensity, $I_s$, to the incident intensity, $I_0$, is given by:

$$I_s/I_0 = \sum K N_i \alpha_i^2/\lambda_0^4 \qquad (12)$$

where $K$ is a coefficient containing transmission and calibration factors, and $\lambda_0$ is the wavelength. Note that polarizability $\alpha_i$ for i-mers is assumed to be $i$ times larger than molecular polarizability $\alpha_1$ [15].

Here we will use the DSMC method to simulate condensation in a free expanding pure argon plume through a sonic orifice, which had experimentally done in AEDC [15] with a stagnation pressure of 250 torr, stagnation temperature of 280 K and orifice diameter of 3.2 mm. The details of DSMC simulation models and techniques are developed in Ref. [8], which can be briefly summarized as follows. The original 2D axisymmetric SMILE code [24] is modified to simulate nucleation, cluster-molecule and cluster-cluster collision, and evaporation processes. The simulation domain extends 4 and 10 times the orifice diameter in the radial and axial directions, with 100 and 250 cells respectively. Each cell can be divided into up to 16 subcells according to the flow gradients obtained during the simulation, and a time step of $2.0 \times 10^{-9}$ s is used. To decrease the computational cost, radial weights are used for distributing the number of simulated molecules evenly in the radial direction for monomers and clusters. A cluster weighting factor of $1.0 \times 10^{-5}$ is used in the simulation due to the several orders of magnitude difference in the cluster and vapor number density. Since the non-condensation region close to the orifice is too dense to be modeled by DSMC, the simulation begins from a starting surface which is created with the continuum solver GASP [25]. About 3,200,000 simulated molecules are used to represent clusters and vapor molecules at steady state. A typical simulation takes 72 hours on 18 parallel AMD Athlon processors of CPU 1526 MHz.

The DSMC simulation results for the condensation plume are shown in Fig. 10, including vapor number density contours (top), cluster number density contours (middle), and average cluster size contours (bottom). It can be seen that the initial cluster or nuclei appear in a nucleation region where cluster number density increases quickly along the flow direction consistent with the increased degree of supersaturation in the free expanding process. Upstream of this region, the gas is essentially an expanding plume without condensation. Further downstream of the nucleation region, cluster number density decreases mainly due to the expansion. Since the cluster number density is only on the order of $10^{17}$ per $m^3$, there are few cluster-cluster collisions so that the importance of the coalescence process on the cluster number density is limited. The average cluster size is usually below 10-mers in the nucleation region, while it increases downstream of the nucleation region due to the sticking collision process between cluster and vapor molecules and cluster evaporation processes.

The distributions of average cluster size, cluster and vapor number density along the core flow are shown in Fig. 11. The figure shows that vapor number density is about 5 orders of magnitude greater than the cluster number density, while the maximum cluster size in the computational domain is about 300-mers. The average cluster size seems to grow continuously beyond the computational domain until the vapor number density becomes so low that the contribution of sticking collisions to cluster growth process counteracts the cluster evaporation effect. The Rayleigh scattering intensity is calculated along the core flow using Eq. (12), and is compared with experimental data in Fig. 12. Note that the dashed line in Fig. 12 indicates the change in Rayleigh scattering intensity along the core of a plume for which condensation is ignored.

Upstream of the nucleation region, there is no condensation in the plume which leads to a Rayleigh scattering intensity decrease along the flow direction due to rarefaction. However, the emergence of clusters and the cluster growth process counteracts the decrease of vapor number density in the condensation region, leading to a scattering intensity downstream of the nucleation region that is larger than its corresponding value in the non-condensation plume. Figure 12 also shows that our numerical results agree reasonably well with the experimental data, thus, we expect the DSMC condensation model may predict the condensation phenomenon in a free expanding plume correctly. Note that the appearance of nuclei in the DSMC simulation is delayed $1.2 \times 10^{-5}$ sec to make the initiation of condensation in the simulation coincide with the onset of condensation at the position indicated in the experiment.

Figure 13 compares the Rayleigh scattering intensity contours between a condensation (top) and non-condensation (bottom) plume. For the non-condensation case, the plume scattering intensity decreases monotonically in the expanding directions, due to the decrease in the vapor number density. However, for the condensation plume, the scattering intensity decreases more slowly in the axial direction after the initiation of condensation. Consistent with the results shown in Fig. 11, there is a counteracting effect between the increase of the cluster size and the decrease of the cluster number density. Our numerical simulation results show that there would be a long tail in the Rayleigh scattering intensity distribution in the free expansion condensation flow. The exact spatial distribution should be further validated by future experiments.

# 5 Summary

The general molecular dynamics (MD) approach is used to verify an analytical cluster model, and cluster sticking collision model. The semiempirical Ashriz-Poo model is used to predict the outcome of cluster-cluster collision. The use of LJ potential reduced units shows that MD simulation results of Argon cluster agree well with those of Nickel cluster done in an other independent work, indicating that the MD results in this work may be approximately transferred to other species.

The MD simulation results are applied into the DSMC model, which is developed to simulate homogeneous condensation in a free expanding Argon plume through a sonic orifice. According to the DSMC simulation results, Rayleigh scattering intensity is estimated and compared with the experimental data suggesting that the condensation model developed in this work may reasonably well predict homogeneous condensation in a free expanding plume. The Rayleigh scattering contours in a condensation plume are predicted, which may need to be validated by experimental data in the future.

# 6 Acknowledgements

The authors wish to express their gratitude to Professor M.S. Ivanov for inspiring this study and to Professor L.V. Zhigilei for providing the computer code. This work was supported by the Air Force Office of Scientific Research Grant No. F49620-02-1-0104 administered by Dr. Mitat Birkan and the Army Research Office Grant No. DAAD19-02-1-0196, administered by Dr. David Mann.

# References

[1] Farid F. Abraham, *Homogeneous Nucleation Theory*, Academic Press, 1974, 263

pages.

[2] J. W. L. Lewis and W. D. Williams, " Profile of an Anisentropic Nitrogen Nozzle Expansion", *The physics of Fluids*, Vol. 19, No. 7, July 1976, pp. 951-959.

[3] M. S. Ivanov, G. N. Markelov, Yu. I. Gerasimov, A. N. Krylov, L. V. Michina, and E. I. Sokolov, " Free-Flight Experiment and Numerical Simulation for Cold Thruster Plume", *Journal of Propulsion and Power*, Vol. 15, No. 3, May-June, 1999.

[4] O. F. Hagena, and W. Obert, "Cluster Formation in Expanding Supersonic Jets: Effect of Pressure, Temperature, Nozzle Size, and Test Gas", *the Journal of Chemical Physics*, Vol. 56, No. 5, 1972.

[5] W. D. Williams and J. W. L. Lewis, "Summary Report for the CONTEST Program at AEDC", AEDC-TR-80-16, Sept. 1980.

[6] E. R. Perrel, W. D. Erickson, and G. V. Candler, " Numerical Simulation of Nonequilibrium Condensation in a Hypersonic Wind Tunnel ", *JSME International Journal*, Series B, Vol. 39, No.2, pp. 277-283, Apr.-Jun. 1996.

[7] G. A. Bird, *Molecular Gas Dynamics and the Direct Simulation of Gas Flows*, Oxford Science Publications, 1994. 458 pages.

[8] Jiaqiang Zhong, Sergey F. Gimelshein, Michael I. Zeifman, and Deborah A. Levin, "Modeling of Homogeneous Condensation in Supersonic Plumes with the DSMC Method", AIAA paper 2004-0166, Jan. 2004.

[9] Quanhua Sun, Iain D. Boyd, and Kenneth E. Tatum, "Particle Simulation of Gas Expansion and Condensation in Supersonic Jets", AIAA paper 2004-2587, Jun. 2004.

[10] M. P. Allen, and D. J. Tildesley, *Computer Simulation of Liquids*, Oxford University Press, 1987. 385 pages.

[11] R. Venkatesh, W. H. Marlow, R. R. Lucchese, and J. Schulte, "The effect of the nature of the interaction potential on cluster reaction rates", *J. Chem. Phys.*, Vol. 104, No. 22, pp. 9016-9026, Jun. 1996.

[12] Michael I. Zeifman, Jiaqiang Zhong, and Deborah A. Levin, "A hybrid MD-DSMC Approach to Direct Simulation of Condensation in a Supersonic Jets", AIAA paper 2004-2586, Jun. 2004.

[13] R. Soto, and P. Cordero, " Cluster Birth-death Processes in a Vapor at Equilibrium", *J. Chem. Phys.*, Vol. 110, No. 15, pp. 7316-7325, Apr. 1999.

[14] V. Bernshtein, and I. Oref, " Dependence of Collision Lifetimes on Translational Energy", *J. Phys. Chem. A*, Vol. 105, No. 14, pp. 3454-3457, 2001.

[15] J. W. L. Lewis and W. D. Williams, "Argon Condensation in Free-jet Expansion", AEDC-TR-74-32, July, 1974.

[16] H. Muller, H. G. Fritsche, and L. Skala, " Analytic Cluster Models and Interpolation Formulae for Cluster Properties", in *Clusters of Atoms and Molecules I: Theory, Experiment, and Clusters of Atoms*, edited by H. Haberland, pp. 115-138, Springer-Verlag, 1995, 422 pages.

[17] Ian M. Withers, " A Computer Simulation Study of Tilted Smectic Mesophases", Sheffield Hallam University, Ph.D thesis, 2000.

[18] C. M. Benson, J. Zhong, S. F. Gimelshein, D. A. Levin and A. Montaser, " Simulation of Droplet Heating and Desolvation

in Inductively coupled Plasma - Part II: Coalescence in the Plasma ", *Spectrochimica Acta - Part B Atomic Spectroscopy*, Vol. 58, n 8, page 1453-1471, Aug. 2003.

[19] B. Briehl and H. M. Urbassek, " Monte Carlo Simulation of Growth and Decay Processes in a Cluster Aggregation Source ", *Journal of Cacuum Science & Technology A*, Vol. 17, n 1, page 256, Jan.-Feb. 1999.

[20] G. K. Schenter, S. M. Kathmann, and B. C. Garrett, " Dynamical Benchmarks of the Nucleation Kinetics of Water ", *Journal of Chemical Physics*, Vol. 116, n 10, pp. 4275-4280, Mar. 2002.

[21] Gyoko Nagayama, Takaharu Tsuruta " A general expression for the condensation coefficient based on transition state theory and molecular dynamics simulation", *Journal of Chemical Physics*, Vol. 118, n 3, pp. 1392-1399, Mar. 2003.

[22] Ashgriz, N. and Poo, J. Y., "Coalescence and Separation in Binary Collisions of Liquid Drops," *Journal of Fluid Mechanics*, Vol. 221, 1990, pp. 183-204.

[23] Benson, C. M. "An Advanced Model for the Determination of Aerosol Droplet Lifetime in an Inductively Coupled Plasma", Ph.D Dissertation, Dept. of Chemistry, George Washington University, 2002.

[24] M. S. Ivanov, G. N. Markelov, and S. F. Gimelshein, "Statistical simulation of reactive rarefied flows: numerical approach and application", AIAA Paper 98-2669, June 1998.

[25] The General Aerodynamic Simulation Program, GASP version 4.1, Computational Flow Analysis Software for the Scientist and Engineer, User's Manual, Aerosoft, Inc. Virginia.

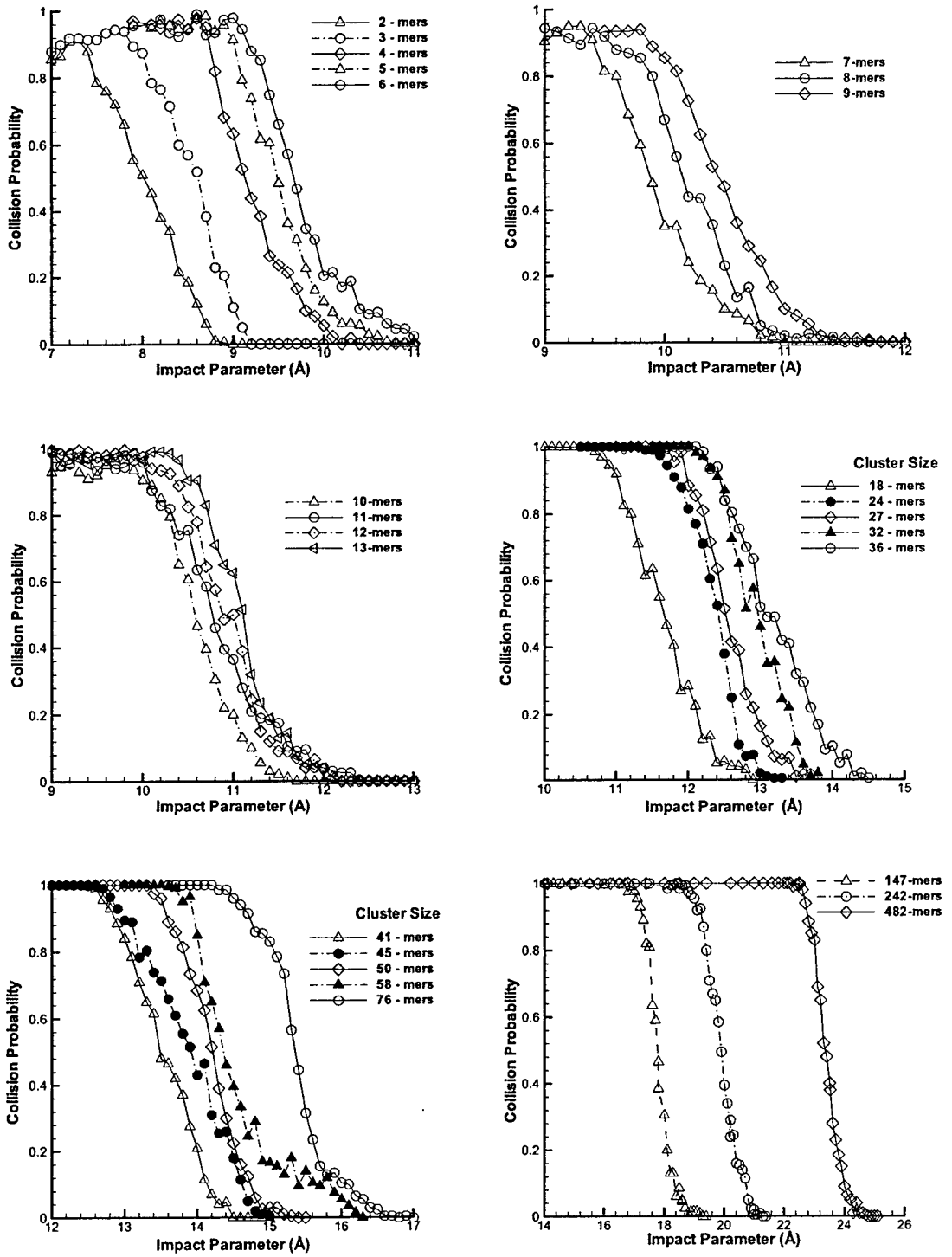


Figure 1: Comparison of collision probability for some clusters from dimer to 482-mers under the condition of various impact parameters, with a relative collision velocity of $182m/s$.

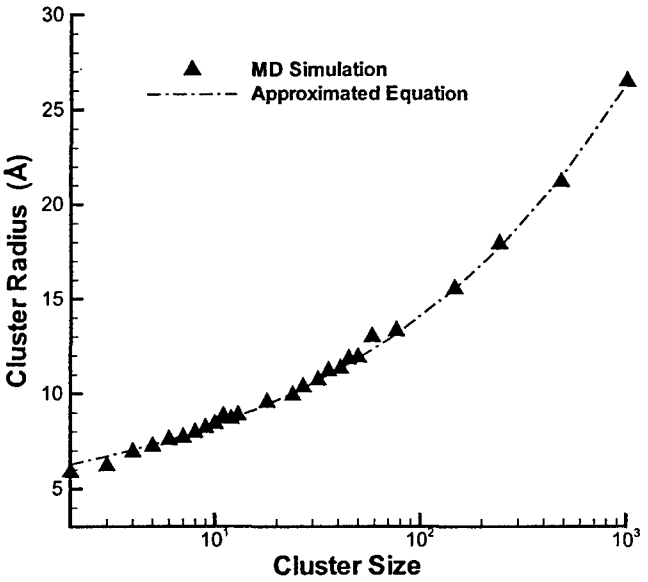


Figure 2: Average cluster radius from MD simulations with a relative collision velocity of $182m/s$ is fitted to an approximated Equation, $R_i = 2.3i^{\frac{1}{3}} + 3.4$.

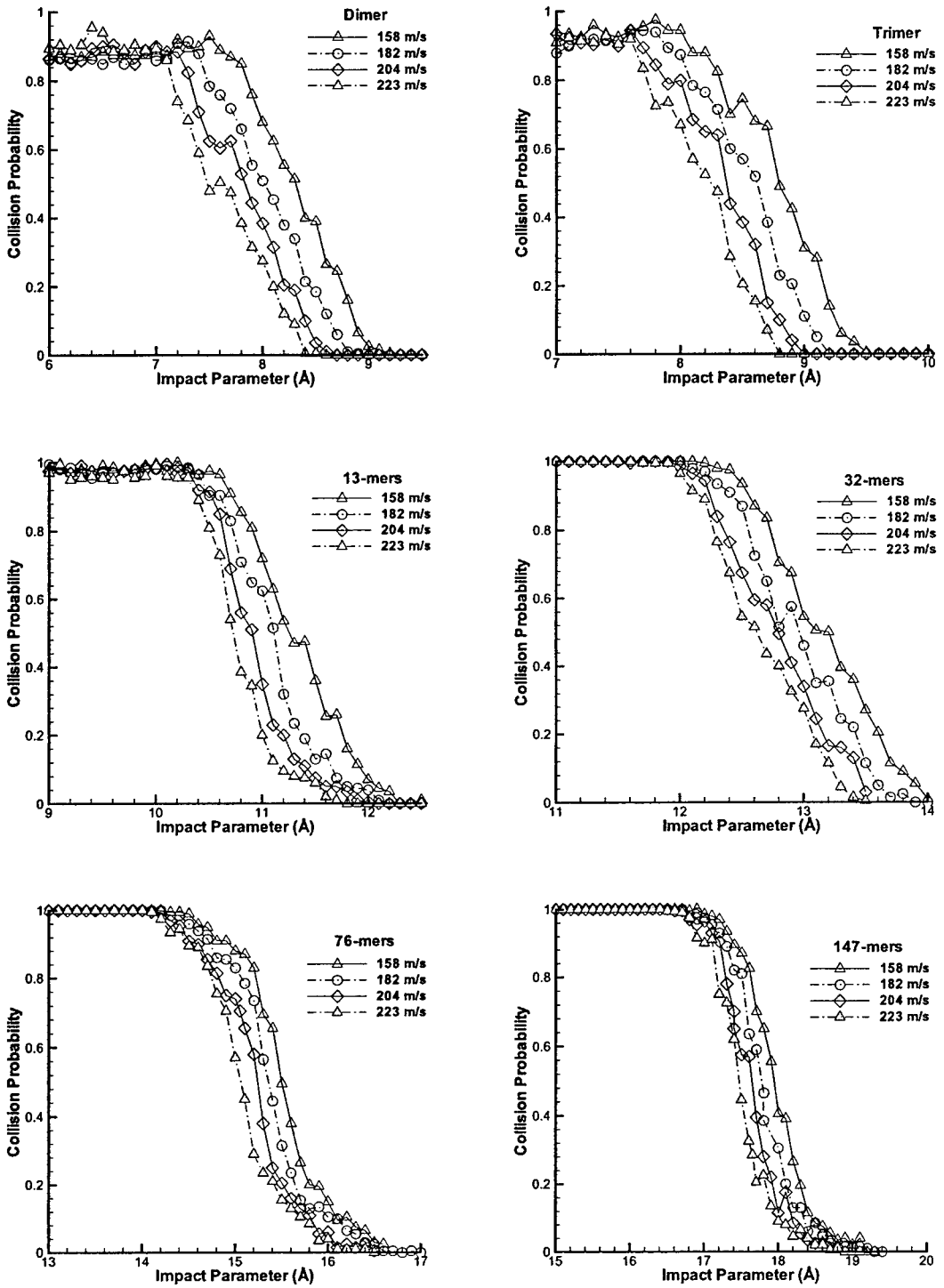


Figure 3: Comparison of collision probability for some clusters under the condition of various impact parameters and relative collision velocities.

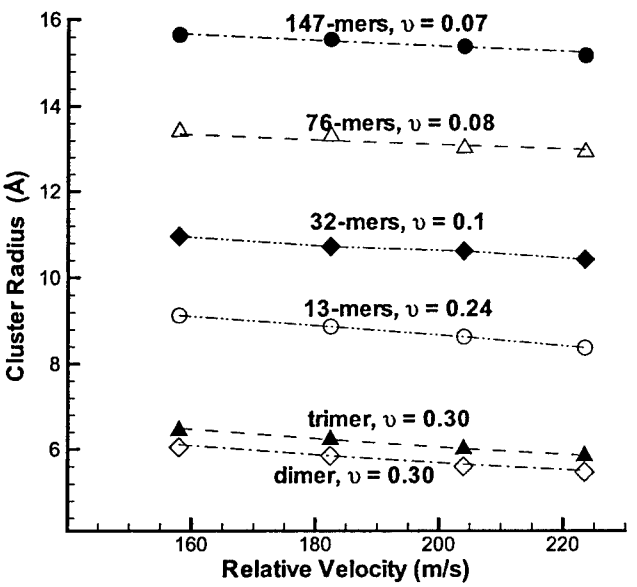


Figure 4: Cluster radius simulated from MD are fitted with equations: $r = r_{ref}(\frac{c_{ref}}{c_r})^{\nu}$.

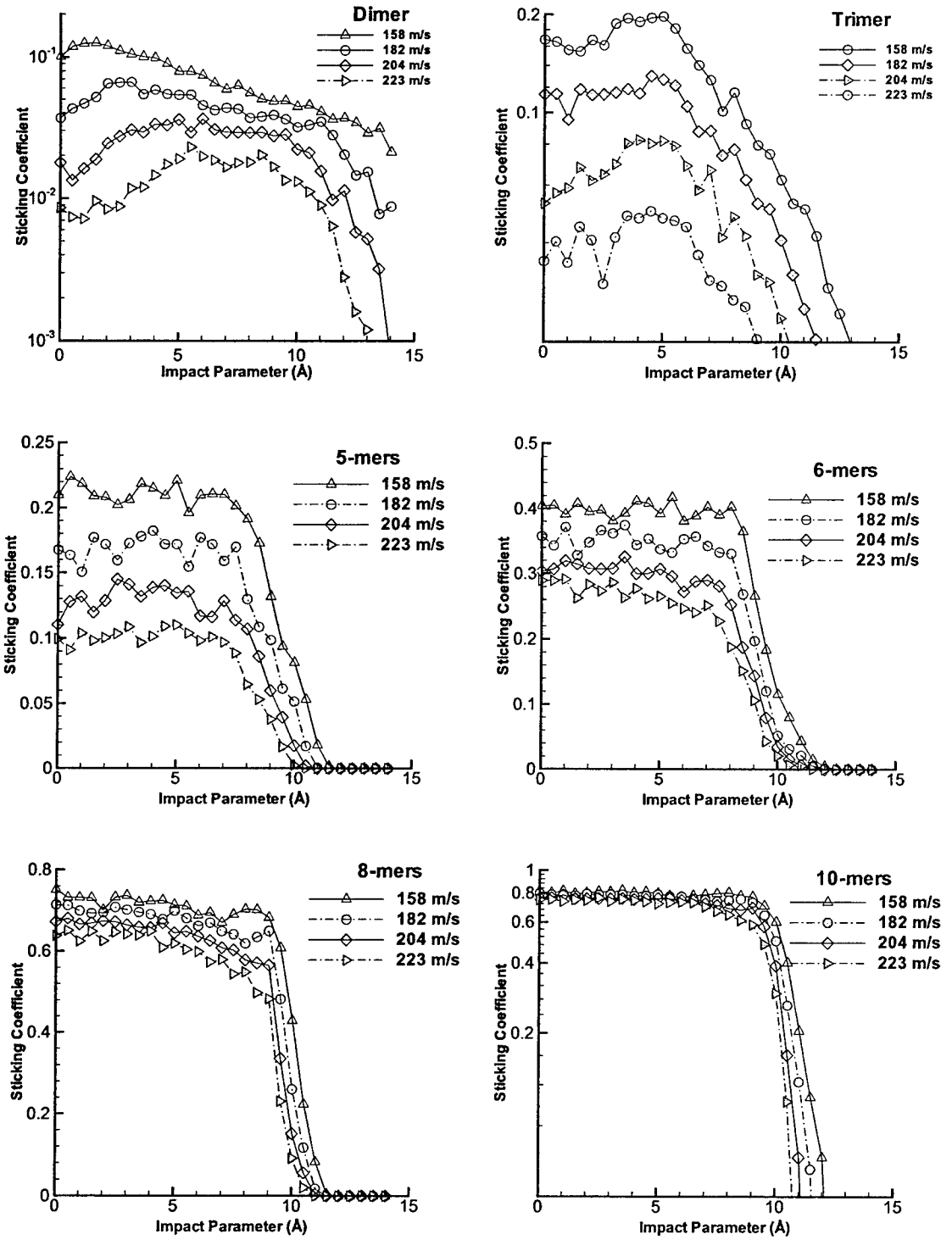


Figure 5: MD simulation results of sticking collision coefficient or probabilities for some clusters under the condition of various impact parameters and relative collision velocities.

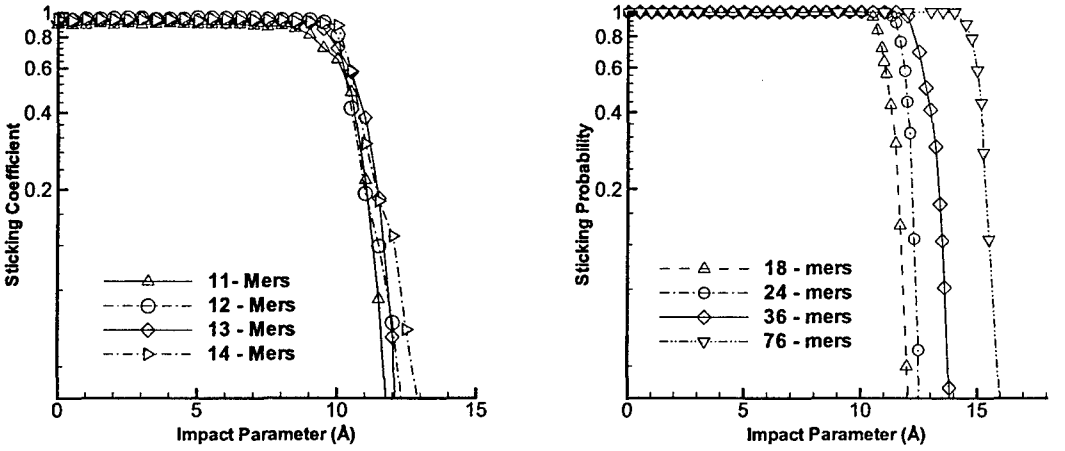


Figure 6: MD simulation results of sticking collision coefficient for clusters of different sizes as a function of impact parameter, with a relative collision velocity of $182m/s$.

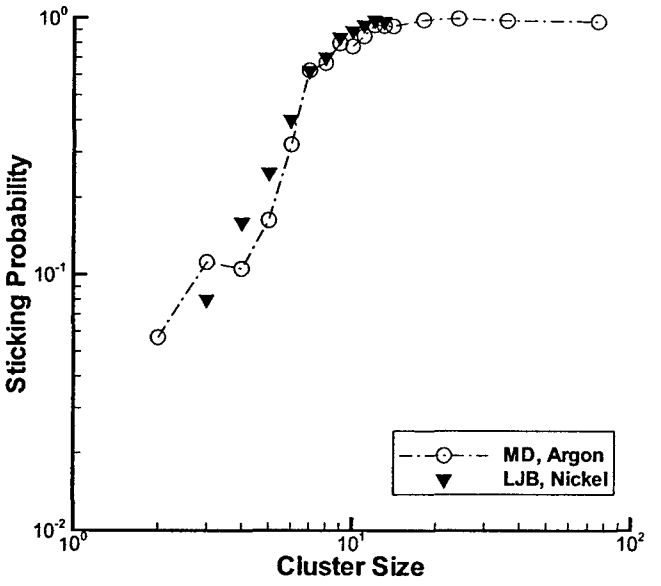


Figure 7: Average cluster sticking probabilities, for argon clusters from dimer to 76-mers with a relative collision velocity at $182m/s$, are indicated by open circles compared with nickel cluster sticking probabilities as solid symbols.

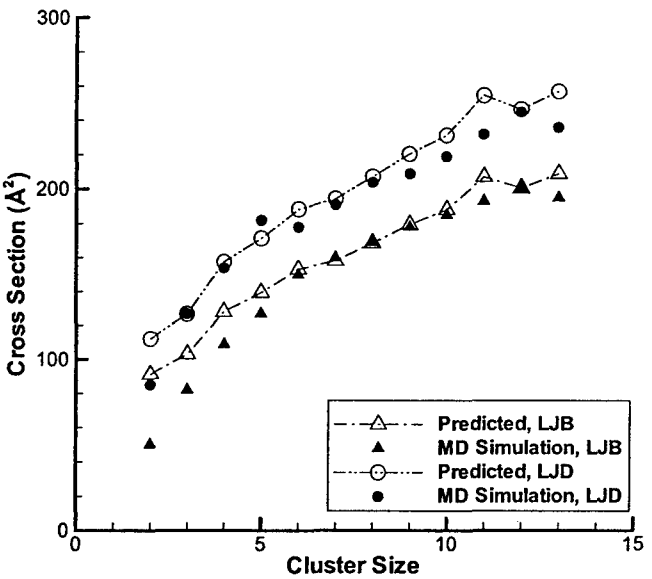


Figure 8: Comparison of predicted nickel cluster cross section from simulated argon clusters using Eq. (6) with MD simulation results.

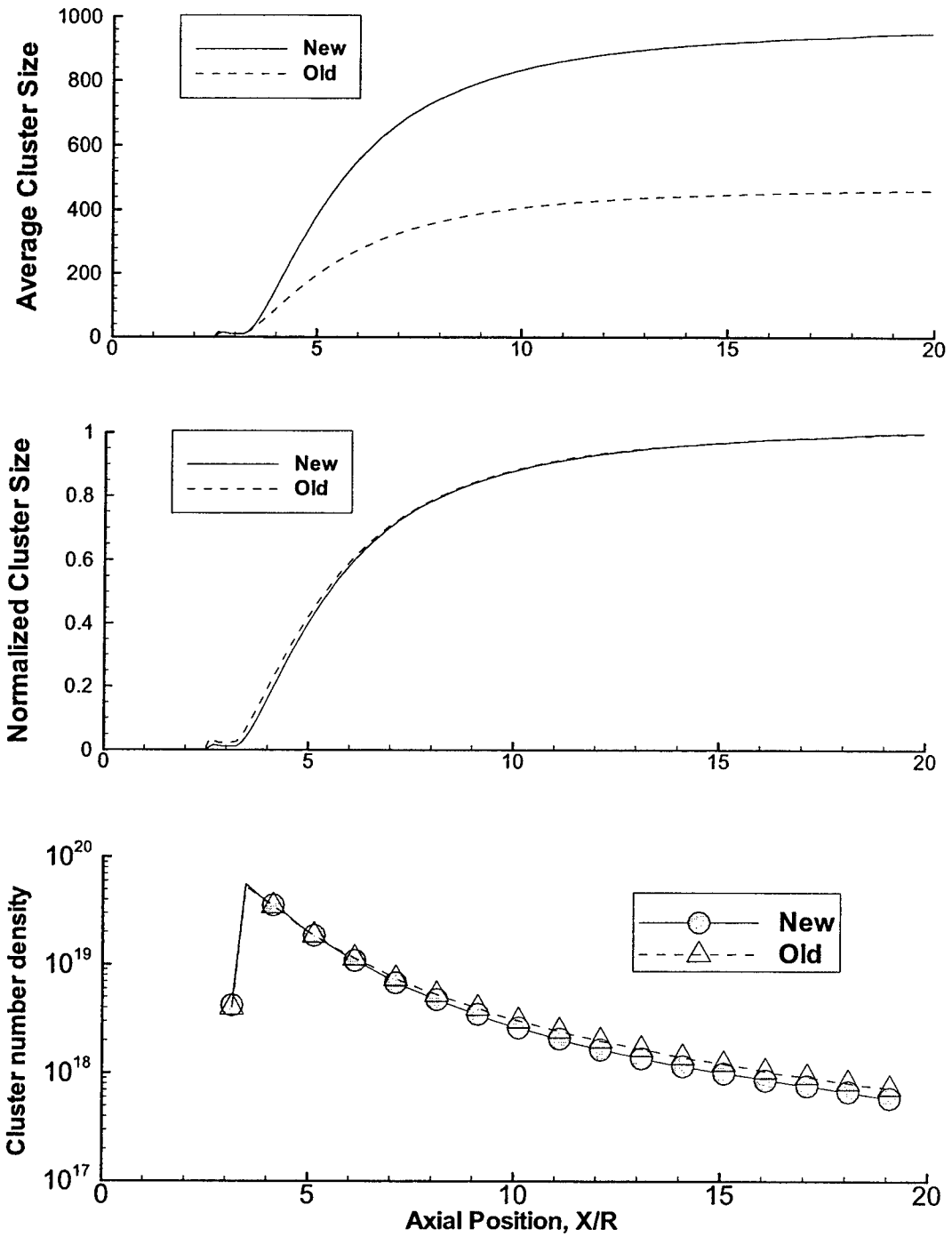


Figure 9: Contours of Ar cluster size (top), normalized cluster size (middle), and cluster number density (bottom) along the plume centerline between the improved (new) and previous (old) results. Number density is given in per $m^3$, Axial position is normalized to the nozzle throat radius $R$.

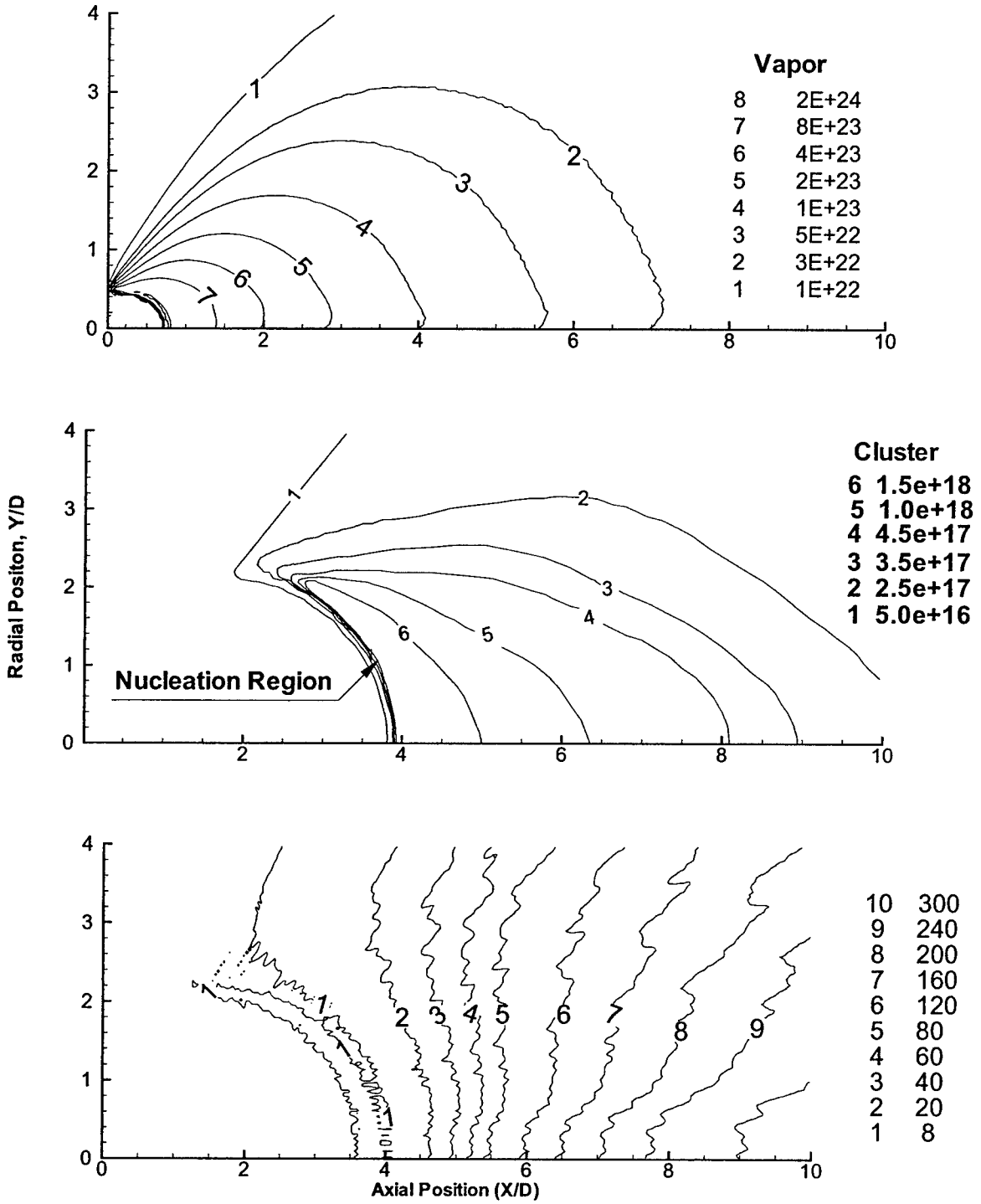


Figure 10: Contours of Ar vapor number density (top), cluster number density (middle) and average cluster size (bottom) in the condensation plume, discussed in Sec. 4. Number density is given in per $m^3$.

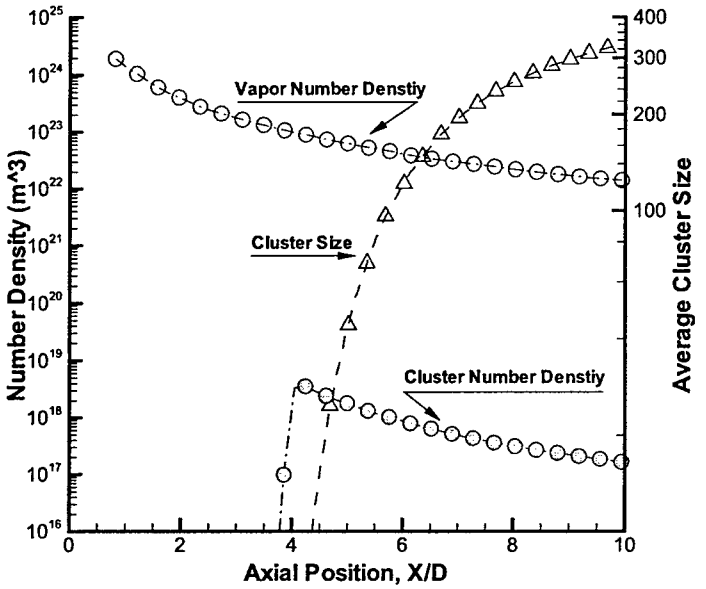


Figure 11: The distribution of Argon gas and cluster number density, and average cluster size along the center line of the condensation plume, discussed in Sec. 4.

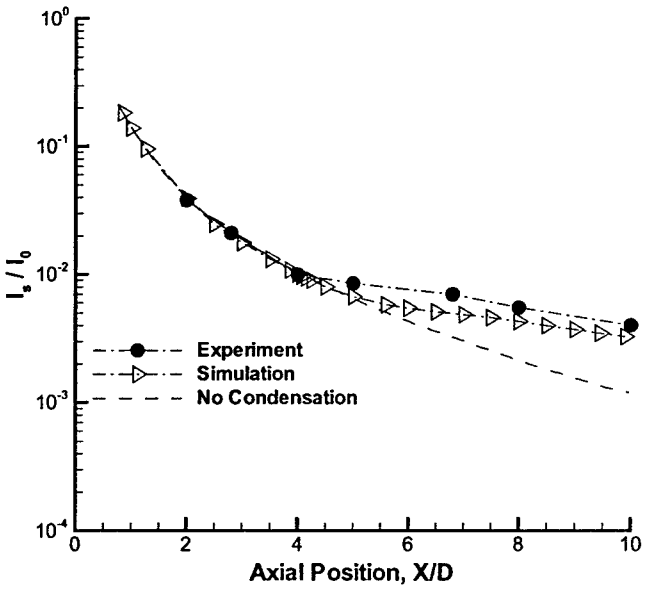


Figure 12: Comparison of Rayleigh scattering intensity between experimental data and simulation results along the plume center line. The dashed line indicates intensity of a flow solution without condensation.

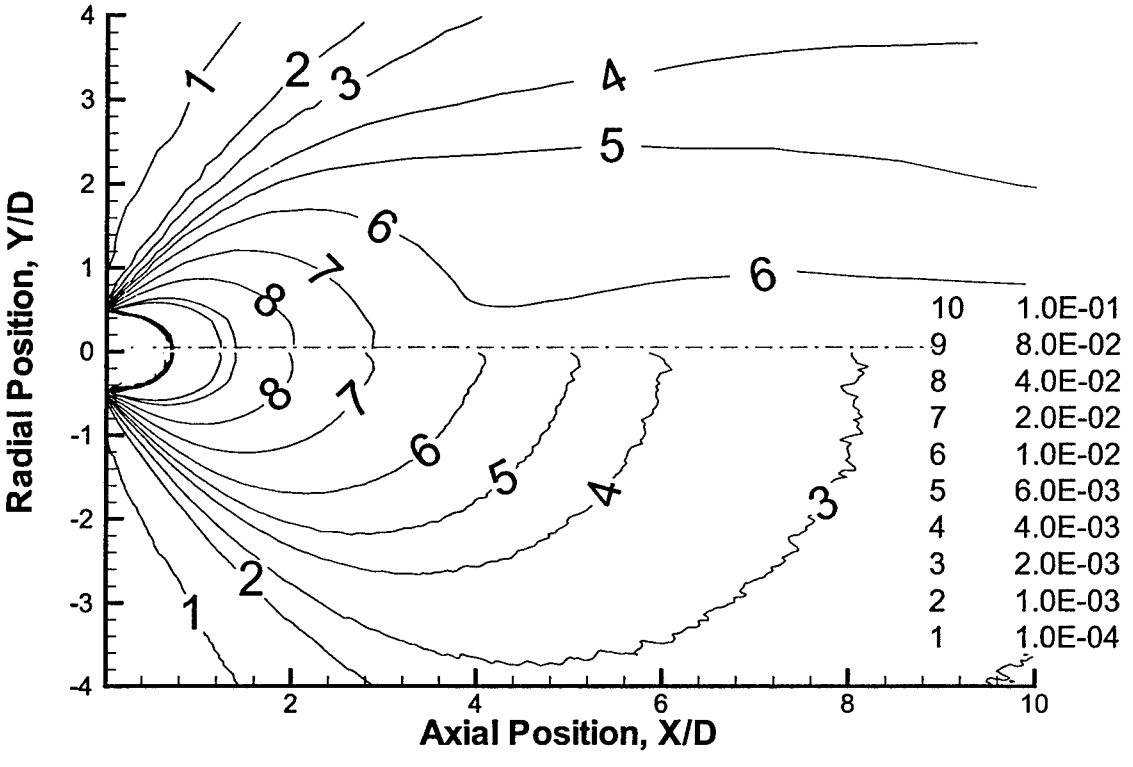


Figure 13: Comparison of Rayleigh scattering intensity contours, $I_s/I_0$, between condensation (top) and plume without condensation (bottom).